International Conference on Space Optics—ICSO 2014

La Caleta, Tenerife, Canary Islands

7–10 October 2014

Edited by Zoran Sodnik, Bruno Cugny, and Nikos Karafolas

Design and performances of the fluorescence imaging spectrometer of flex

D. Dubet

P. Crescence

C. Miesch

D. Lobb

DESIGN AND PERFORMANCES OF THE FLUORESCENCE IMAGING SPECTROMETER OF FLEX

D. Dubet[1], P. Crescence[1], C. Miesch[1], D. Lobb[2]

[1]*Airbus Defence and Space, France. [2]Surrey Satellite Technology Limited, United Kingdom*

I.   INTRODUCTION

The FLuorescence EXplorer (FLEX) mission is one of the two candidates of ESA's 8th Earth Explorer opportunity mission. A system feasibility (Phase A/B1) study is about to be completed. The FLuORescence Imaging Spectrometer (FLORIS) is an imaging spectrometer on board of a medium sized satellite flying in tandem with Sentinel-3 in a Sun synchronous orbit at a height of about 814 km. FLORIS will observe vegetation fluorescence and reflectance within a spectral range between 500 and 780 nm, allowing the monitoring of seasonal variations of the vegetation cycles. FLORIS observes the land area including coastal zones (50 km).

FLORIS includes two channels at high (0.3 nm) and low (2 nm) spectral resolutions with a spectral oversampling of a factor 3. It offers a ground spatial sampling of 300 m for a swath width of 150 km.

II.   MAIN REQUIREMENTS FOR FLEX/FLORIS

The FLEX/FLORIS major requirements are provided in Table 1.

Table 1: FLEX/FLORIS main requirements

Requirement	Specification	Comment
Instrument type	Pushbroom Imaging Spectrometer	
Mission lifetime	3.5 years (T) / 5 years (G)	
Data latency	5 h (T) / 24 h (G)	
Coverage	-56°< latitude < 75°	Sun Zenith < 75° , Observation Zenith < 15°
Pitch angle	< 5°	Preferably Nadir pointing
Swath width	150 km	Enables global coverage
Spatial Sampling Distance (SSD)	300 m	At Nadir
System Integrated Energy (SIE)	>70%	over an area of 1.1 SSD ALT x 1 SSD ACT
Spectral band coverage	See Fig. 1	
Spectral Resolution and Sampling	See Fig. 1	
Signal to noise ratio	See Fig. 2	
Spectral stability	1 nm 10 pm (HR) ; 0.1 SSI (LR)	Over mission lifetime During observational time of 1 orbit
Stray light sensitivity	See Fig. 3	Specified on non-uniform scene
Spectral co-registration	<0.1 SSD	Smile
Spatial co-registration	<0.1 SSD	Keystone
Knowledge of ISRF	Better than 1%	Instrument Spectral Response Function
Absolute radiometric accuracy	2% (G) 3% (T)	Excluding uncertainty of Sun radiance
Relative radiometric accuracy	1%	Spectral and spatial
Polarisation sensitivity	2% (LR); 1% (HR)	
Temporal co-registration	6s (G) / 15s (T)	To avoid significant cloud movements
Inter-channel temporal co-registration	< 2s	
Geo-location accuracy	0.3 SSD	

T: Threshold value G: Goal value

The FLEX/FLORIS spectral requirements are defined in Fig. 1. The spectral bands with high spectral resolution are the two Oxygen bands O2A and O2B. The spectral bands with low spectral resolution are the Photochemical Reflectance Index (PRI), the Chlorophyll Absorption and the Red Edge bands. The Spectral Resolution (SR) and the Spectral Sampling Interval (SSI) are provided in Fig. 1
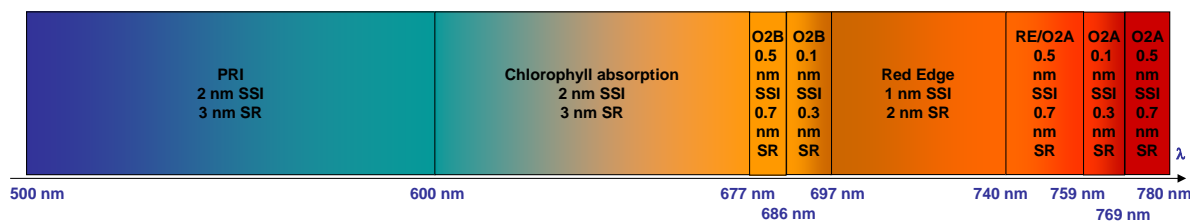
Fig. 1. FLORIS spectral requirements

The Signal to Noise Ratio (SNR) is specified for each spectral band in Fig. 2. The SNR is defined for a spectral interval equal to the SR.

	PRI	Chlorophyll absorption	O2B		Red-edge		O2A		
λ min (nm)	500	600	677	686	697	740	755	759	769
λ max (nm)	600	677	686	697	740	755	759	769	780
SR (nm)	3	3	0.7	0.3	2	0.7	0.7	0.3	0.7
SSI (nm)	2	2	0.5	0.1	1	0.5	0.5	0.1	0.5
SNR	300	300	400	300	600	1200	1200	200	1200

Fig. 2: FLORIS SNR requirements

The stray light is specified not to affect the absolute radiometric accuracy of the reference radiance in a non-uniform scene with the presence of clouds. The non-uniform scene is defined in Fig. 3 where the inner part at the reference radiance has a width of 20 (G) or 40 (T) SSD. The radiometric error generated by the stray light at the central point of the inner part must be compatible with the requirement of absolute radiometric accuracy.
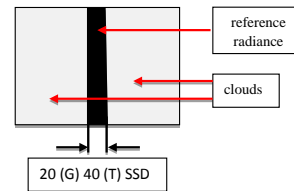

Fig. 3: Non uniform scene for stray light requirement

III.   OVERALL DESIGN

The analysis of the spectral requirements has led to define two distinct channels:
-   A High spectral Resolution (HR) channel with a spectral resolution of 0.3 nm and a spectral sampling of 0.1 nm covering the O2B band (677-697 nm) and O2A band (740-780 nm)
-   A Low spectral Resolution (LR) channel with a spectral resolution of 2 nm and a spectral sampling of 0.667 nm covering the PRI band (500-600 nm), the chlorophyll absorption band (600-677 nm) and the Red Edge band (697-740 nm); in fact the LR channel covers the full spectral range (500-780 nm) allowing a cross correlation with the HR channel

Both channels provide a spectral oversampling of a factor 3, thanks to a 84 µm wide slit and a pixel size of 28 µm along the spectral direction. The telescope focal length is 228 mm to scale the 300 m on ground SSD on the 84 µm slit width for the altitude of 814 km. The spectrometer has a magnification of 1.The pixel size on the spatial direction is 84 µm got by a binning of 2 pixels of 42 µm. The slit length and the ACT detector size are 42 mm to cover the 150 km swath width.

The need of pupil diameter to comply the SNR requirement is 80 mm (f/2.85) for the HR channel and 40 mm (f/5.7) for the LR channel. The 2 channels are provided by 2 separated instruments allowing a better optimization of the channel optical designs while the co-registration requirement is complied. A common detector with 1000 rows x 430 columns and 42 µm x 28 µm pixel pitch is used for O2A and O2B bands in HR channel and for the LR channel.

The design includes polarization scramblers at telescope entrances of both channels and a common calibration and shutter mechanism. The functional block diagram of the FLORIS instrument is provided in Fig. 4.
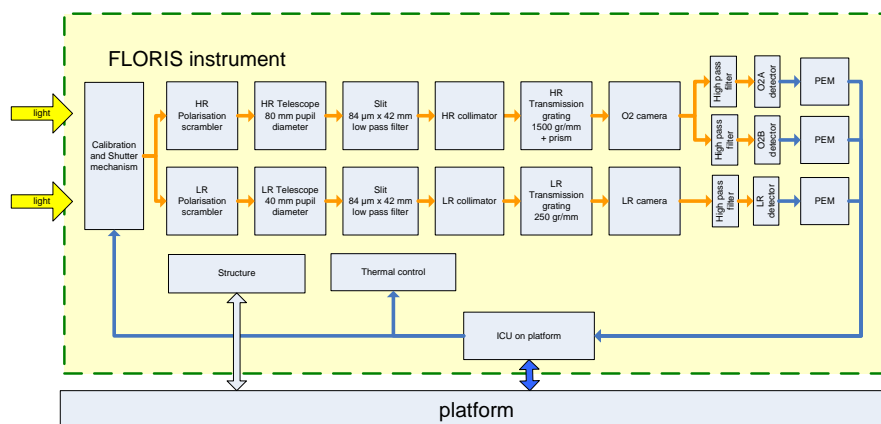

Fig. 4: FLORIS instrument functional block diagram

IV.   OPTICAL CONCEPT

The FLORIS optical system comprises two separate imaging spectrometers, boresighted to cover the same swath width – 150km wide from a nominal altitude 814km – at 300m ground spatial sampling distance (SSD):

- A high-resolution (HR) system providing 0.3 nm spectral resolution over two separate spectral bands: 740 nm to 780 nm and 677 nm to 697 nm (covering the O_2A and O_2B atmosphere absorption bands),
- A low-resolution (LR) system providing 2 nm spectral resolution over the spectral band 500 nm to 780 nm.

The spatial sample interval for both systems, at both the entrance slit and the detector, is 84 µm, with x 2 oversampling provided by 42 µm detector row widths. Detector column widths of 28 µm provide spectral samples averaging 0.1 nm in the HR system and 0.667 nm in the LR system.

A. Optical design

The HR optical design is shown in Fig. 5. The system uses refracting lenses for all imaging tasks: telescope, collimator and camera. The telescope has an external entrance pupil, 80 mm diameter, and 228 mm focal length; it forms an Earth image on the spectrometer entrance slit, which is 42 mm long and 0.084 mm wide. Colour-glass filters are located (a) immediately after the entrance slit and (b) before the two detectors, cutting off wavelengths < 620 nm for the detector assigned to the O_2B band, and < 680 nm for the O_2A band. The first filter, which is tilted 7^0 to control stray reflections, carries a dielectric filter cutting off wavelengths > 810 nm.

The beam from the slit is collimated, passes through a prism and a flat transmitting diffraction grating, and is then focused onto the detector by the camera lens. The camera and collimator lenses are identical in design (each 154 mm focal length) for convenience in manufacture, together working at unit magnification. The collimator forms a pupil image on the grating. The grating has a frequency 1500 cycles/mm, and operates in Littrow condition, in the 1st order, for the mid-wavelength (728.5 nm) of the HR range. The prism is included to correct "smile" distortion of the image (curvature of the image of the entrance slit) produced by the grating. As indicated in the lower diagram of Fig. 5, the design includes a polarisation scrambler and a flat fold mirror in front of the telescope; the fold mirror allows the major axis of the optical system to lie in a plane orthogonal to the nadir (Earth-view) axis. The overall length of the HR optics, including the fold mirror and image area, is 991mm.

The LR optical design is shown in Fig. 6. The principle and general shape of the LR system is similar to that of the HR system, but the system has a smaller (40 mm) aperture and much wider spectral range. As for the HR system, it includes a polarisation scrambler and a flat fold mirror before the telescope. The tilted filter following the entrance slit is a colour glass cutting off below 450 nm; as for the HR optics, it carries the dielectric coating cutting off at wavelengths > 810 nm. The diffraction grating has frequency 254 cycles/mm, and operates in first order. No prism is included in the LR system, for which smile correction is not a priority. The LR detector is tilted 13.70° for chromatic correction. Overall length of the LR optics, including fold mirror and image area, is 872 mm.
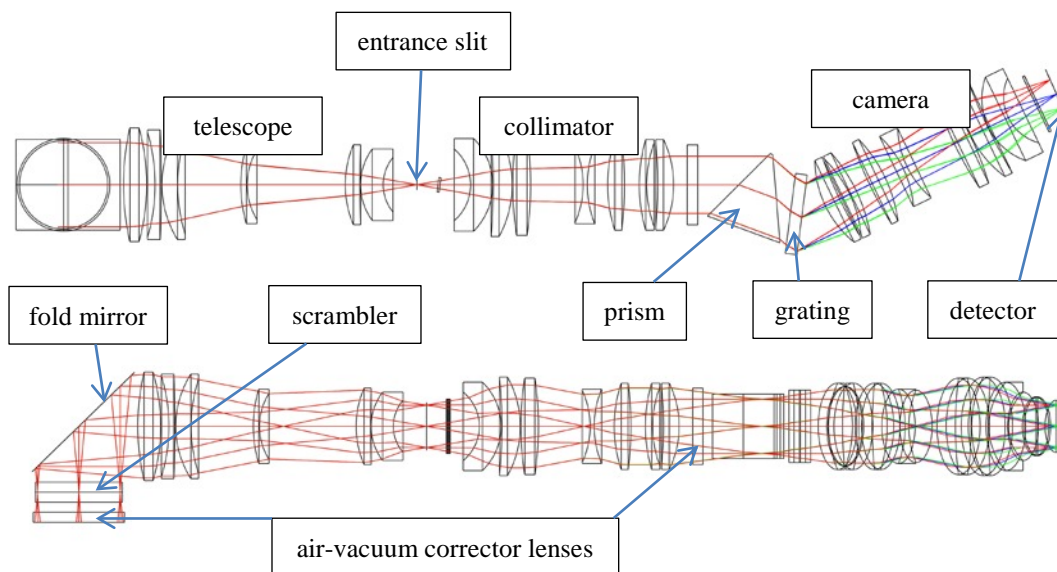

**Fig. 5 High-resolution optical system: views on nadir axis (upped diagram) and across-track (lower)**
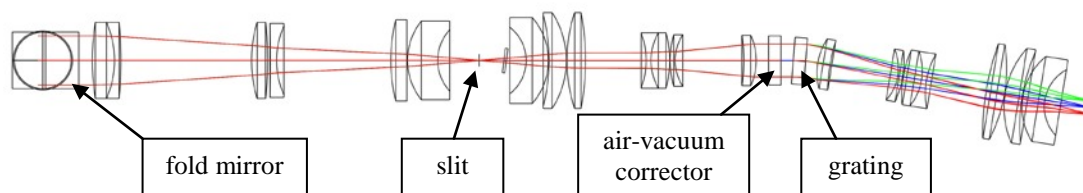
Fig. 6 Low-resolution optical system: view on nadir axis

B. Optical performances

There are stringent requirements on enclosed energy for the optical systems, so that spot sizes at the entrance slit and detector must be small fractions of the 84 µm spatial resolution element corresponding to the ground sample distance, with current targets for rms spot diameters in the region 20 µm. Spectral resolution is less critical, but spreading of the entrance slit image at the detector will also preferably be a small fraction of the 84 µm spectral resolution element. Design performance is indicated in Table 1, in terms of the root-mean-square diameters of point spread functions, respectively on across-track, along-track and spectral axes. Table 2 also shows the design correction for "frown" and "smile" distortions of the image on the detector. Frown is peak-valley error in spatial registration of the spectral samples of each point on ground, which is required to be < 10% of the GSD for the combined HR and LR instrument (including boresight errors). Smile correction, which is important for the HR sub-system, is peak-valley departure of the monochrome slit images from parallel straight lines (it is optimized at 761 nm, where it has a design value 1.9 µm).

Table 2 in general gives worst-case design performance for all field angles and wavelengths. The low-resolution system is significantly more difficult, in spite of smaller aperture, due to chromatic aberrations, since a wide spectral range is covered using glasses limited to available radiation-resistant types. Design performance with air-vacuum corrector lenses (in air) has very little effect on performance with respect to design performance in vacuum. Detailed tolerance analysis indicates that tight controls on optics manufacture, including for example control on lens surfaces tilts to around 7 µm run-out, will introduce changes in rms spot diameters in the region of 10 µm (typically to be added to design diameters on a root-sum-square basis), and changes in spatial registration errors in the region of 3 µm. The optical systems are close to athermal with typical selections for mounting structure materials, so that temperature changes are expected to have relatively small effects.

Table 2 Design performance of FLORIS optics

Parameter	HR optical system	LR optical system
Along-track rms spot diameter at slit	6 µm	11 µm
Across-track rms spot diameter at detector (all optics)	7 µm	8 µm
Spectral rms spot diameter (spectrometer only)	9 µm	15 µm
Bow of spectral line image (smile)	<4.2 µm	0.24 mm to 0.29 mm
Intra-band spatial registration (frown)	0.5 µm	0.7 µm
Inter-band peak-valley spatial registration error	0.7 µm (dominated by LR optics)	
Spatial sample on ground (84µm at detector)	300.0 m to 303.7 m	
Spectral sample interval (28µm at detector)	0.090 nm to 0.108 nm	0.697 nm to 0.704 nm

C. Stray light performances

Stray light analysis of FLORIS optics has concentrated on the HR system, which aims to detect fluorescence as anomalous radiance in the Oxygen absorption lines: performance is critically affected by stray light reaching the detector columns dedicated to low spectral radiance levels, generally including "spectral" stray light from high-radiance spectral regions. The general target for stray light control – stray-light radiance errors < 1% of true radiance – is most difficult to achieve at the 761nm O_2A absorption line. Analysis using Zemax and FRED software has indicated that errors of several percent are likely to be generated at 761nm – the dominant contributors are (a) scatter from particulate contamination on optical surface and (b) scatter due to imperfect polish of optical surfaces. Diffraction at the telescope aperture has significant effects, however these are limited to dark scene areas very close to bright areas. Effects of structure scatter are predicted to be negligible, and double reflections between optical surfaces (ghosts) will produce only minor contributions, assuming feasible

performance of anti-reflection coatings. Errors generated by optics in the spectrometer (entrance slit to detector) are much more significant than errors due to telescope optics (due to the spectral filtering effect of the spectrometer on the telescope image).

The stray light analysis programs work by tracing large numbers of rays. They tend to give very noisy results for the low-angle scatter effects with which we are mainly concerned (including particulate scatter and imperfect-polish scatter) since high intensity scatter close to the specular direction is inadequately sampled in acceptable run-times. Recent analysis has therefore been based on "kernel" analysis, in which the stray light point spread functions at the entrance slit and detector planes are convolved with nominal image-irradiance distributions to generate stray irradiance distributions.

A typical result for particulate contamination in the HR spectrometer (optics from the entrance slit to the detector) is shown in Fig. 7. The diagram on the left shows a spectral radiance distribution input at the entrance slit, limited to the spectral range 680 nm to 810 nm defined by filters in the HR O_2A band. (Wavelengths are on the axis obscured by the surface plot.) The deep atmosphere absorption band is clearly visible. For a critical stray light assessment, scene spectral radiance is specified at two levels, representing respectively a reference scene (for which the 1% stray light target is defined) and top-of-cloud. The defined scene is at cloud radiance across 500 resolved spatial samples, except for a 40-sample wide band in the centre of the swath, which provides a reference-radiance target. In the O_2A band, cloud radiance is typically 3x reference radiance. The diagram on the right in Fig. 7 shows stray light errors for this scene as percentages of true radiance levels. The wavelength indices represent wavelengths from 740 nm to 780 nm. Percent errors show peaks at the deepest absorption line (761 nm in the spectral domain) and of course in the spatial band at reference radiance. In the centre of the reference radiance band, and at 761 nm, the errors reach 2%, due only to particulate contamination.

For this analysis, particulate contamination levels are generally set at 10 ppm for lens surfaces that are effectively sealed within assemblies, and 50 ppm for other surface. Errors due to imperfect polish have been calculated on the general assumption that scatter can be treated as a 0.5 nm rms roughness on each optical surface (using Harvey-Shack A, B, g functions with B = 10^{-5} and g = 2). On these assumptions, which in practice demand a super-polish to eliminate sub-surface cracks, the effects of imperfect polish are around ¼ of the effects of particulate contamination. Preliminary estimates for grating scatter add a similar error.

It has been established that a feasible narrow-band filter, or a wavelength-graded filter, set close to the detector – particular for the purpose of protecting the O_2A absorption region – can be expected to reduce the worst-case total stray light errors by a factor around 3. However, it is likely that the required performance will demand detailed characterization of the stray light functions of flight hardware, and data correction for stray light errors by data processing on ground.
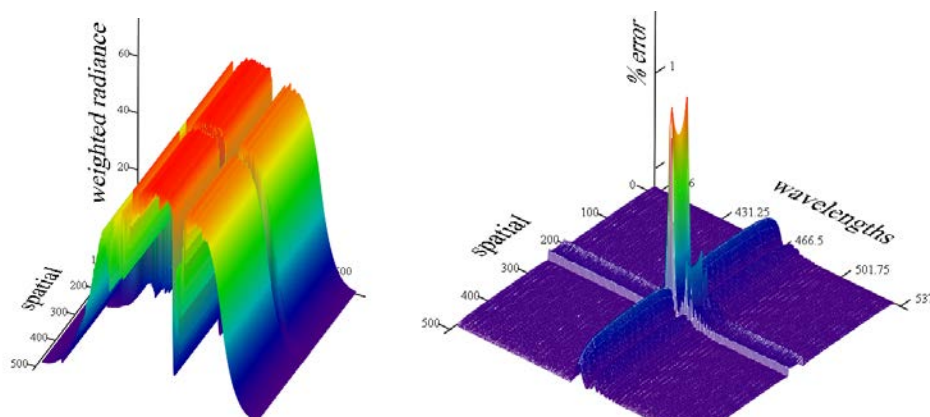

Fig. 7: **Results of stray light analysis – spectrometer particulate contamination**

V.   DETECTION CHAIN

The FLORIS detector is shown in Fig. 8. It is a split frame transfer with parallel transfer in the spatial way. The detector is thinned and back-illuminated, with an optimized anti reflection coating deposition. It uses standard epi thickness and resistivity (16 μm, 100 Ω.cm). It is operated in Non Inverted Mode. The useful area is 1000 x 430 pixels (size of spectrum, without alignment margins); The pixel size is 42μm ACT (pitch between two rows) x 28μm ALT (pitch between two columns). A binning of 2 rows is performed in the serial register before

serial readout to recover the nominal SSD of 300m. The serial register sized to hold 1.9 Me-. The output speed is 3 MPix/s. The detector operating temperature is 263K. The parallel transfer frequency is about 800 kHz.
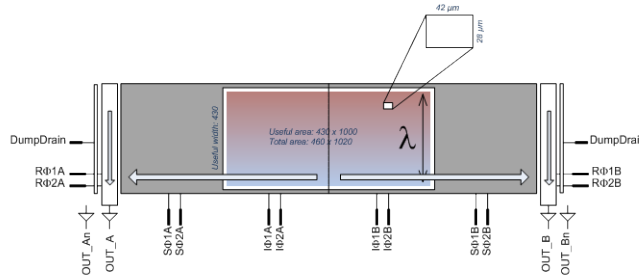

Fig. 8 FLORIS detector

The HR focal plane with the 2 detectors, the Printed Circuit Boards (PCB), the flexure cables and the Proximity Electronics Modules (PEM) is shown in Fig. 9.

The focal plane assemblies of both channels with the radiators for detectors and PEM are depicted in Fig. 10.

The overall functional and electrical architecture of the instrument is provided in the diagram of Fig. 11.

The PEM is in charge of the complete operation of one detector with biasing, sequencer, clocks level translation, video chain implementation and data conditioning towards the Instrument Control Unit (ICU).

The ICU is the unit in charge of the interface between FLORIS and the platform, and drives the different subsystems of FLORIS. The ICU is made of three independent boards, powered by dedicated power lines and with their own command/control remote terminal.
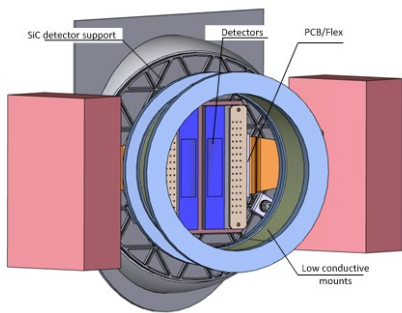

Fig. 9: HR focal plane
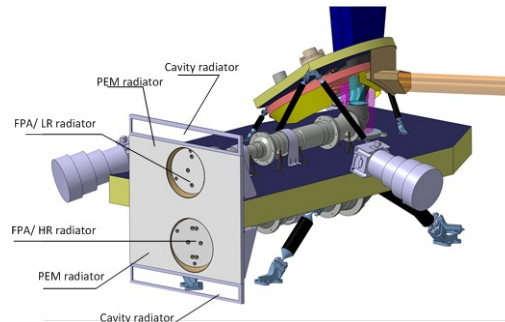
**Fig. 10: Focal plane assemblies**
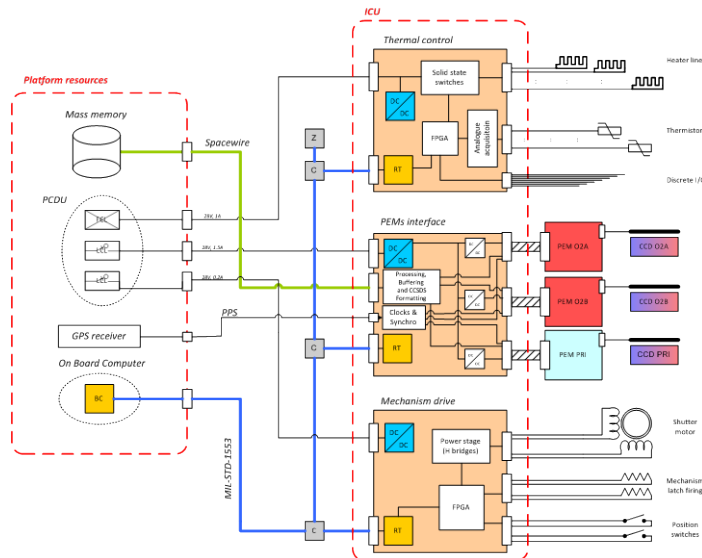
Fig. 11: FLORIS electrical architecture

VI.   CALIBRATION

The radiometric calibration is performed using sun diffusers, one for each channel. The diffusers are installed on a rotating wheel which provides two apertures for the imaging mode and also an opaque portion for shutter mode. The design of the calibration and shutter mechanism is shown in Fig. 12.
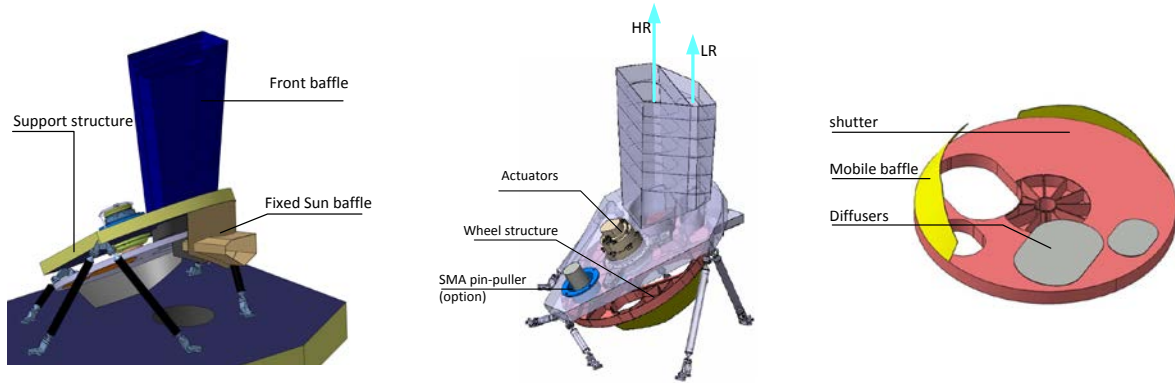

Fig. 12: FLORIS calibration and shutter mechanism

VII.   INSTRUMENT ACCOMMODATION

Both channels are accommodated in an horizontal configuration on the top (HR) and bottom (LR) of a common optical baseplate as illustrated in Fig. 13. The two beams are folded by 2 flat mirrors in order to orientate the lines of sight towards Nadir and to get the entrance beams close to each order in order to use a common calibration and shutter mechanism as shown in Fig. 15. Each channel has a polarization scrambler close to its entrance pupil. Three star trackers are fixed on the instrument baseplate in order to improve the geo location as shown in Fig. 14. The design includes an enclosure to protect from contamination and from radiation and an external multilayer tent to insulate the instrument. The instrument is decoupled mechanically and thermally from the platform thanks an isostatic mounting made of three low conduction bipods. The accommodation of the FLORIS instrument on the platform is shown in Fig. 16
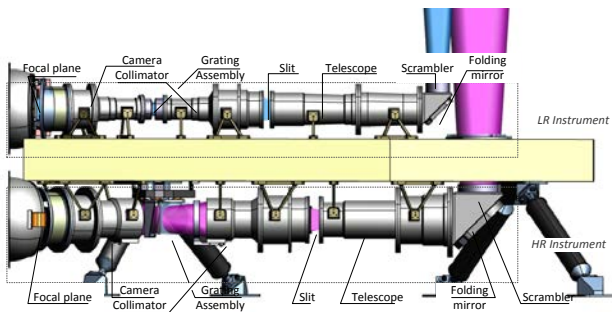

Fig. 13: FLORIS instrument optics accommodation
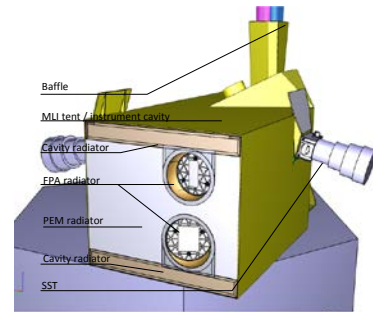
Fig. 14: FLORIS instrument external view
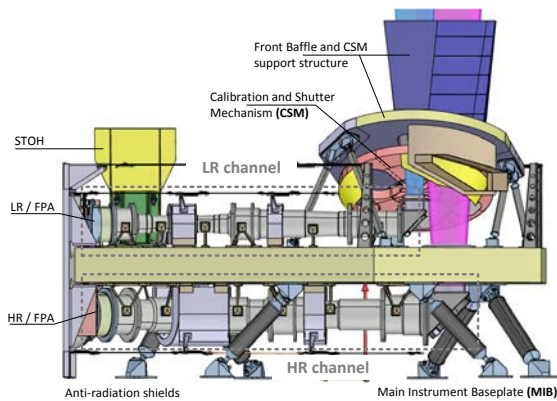
Fig. 15: FLORIS instrument overall design
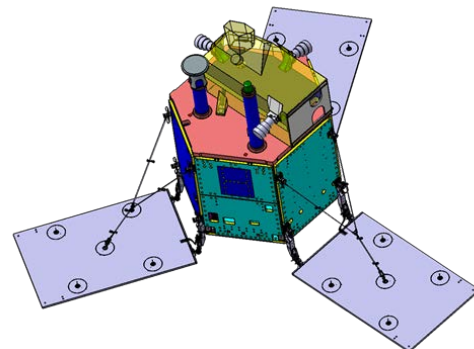
Fig. 16: FLORIS accommodation on platform

VIII. INSTRUMENT MAJOR PERFORMANCES

The radiometric performances in terms of Signal to Noise Ratio (SNR) are shown in Fig. 17. The SNR requirements are met in all channels.


| O2A channel | O2B channel | LR channel |
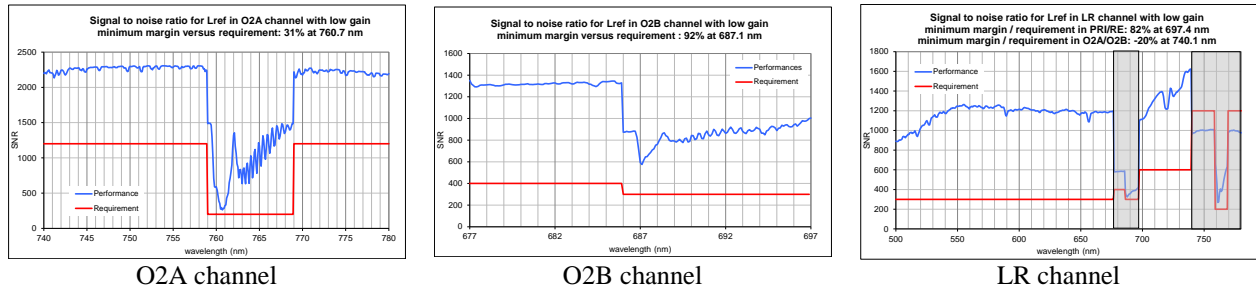
Fig. 17: Performances of Signal to Noise Ratio for the three bands

The System Energy Distribution Functions (SEDF) are provided in Fig. 18. The related System Integrated Energy (SIE) in 1.1 SSD x 1 SSD are 71.4% and 69.8% for the HR and LR channels respectively. The Instrument Spectral Response Functions (ISRF) are provided in Fig. 18. The Spectral Resolutions (SR) defined as the Full Width at Half Maximum (FWHM) are 0.3 nm and 2 nm for the HR and LR channels respectively.


| HR channel | LR channel |
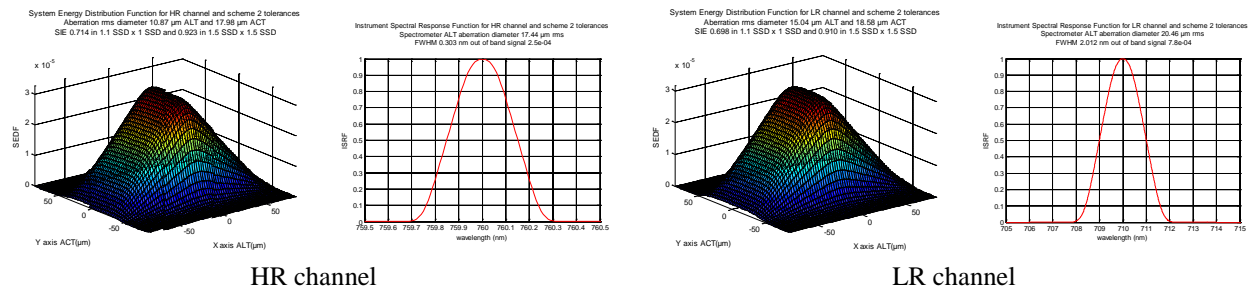
Fig. 18: System Energy Distributions Functions and Instrument Spectral Response Functions

IX. FLEX OBSERVING SYSTEM SIMULATOR

The Observing System Simulator (OSS) models the global response of the FLEX system including the FLORIS instrument up to level 1b products. The OSS is intended to be integrated into an external mission performance End-to-End Simulator (E2ES), which aims to assess mission feasibility and performance with realistic products. The OSS architecture is built in consistence with the foreseen architecture of the E2ES. The OSS architecture considers thus three main modules that can be easily integrated in the E2ES framework, as outlined in Fig. 19.
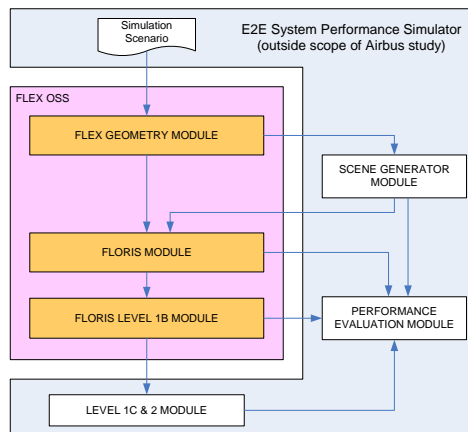

Fig. 19: Overall architecture of the End-To-End Simulator of FLEX, in which the OSS is embedded.

The OSS calculations start with the acquisition grid that accounts obviously for orbitography and platform motion, but also for instrument specific aspects such as multiple slits design and detectors alignment errors at focal plane level (keystone).

The FLORIS module then deals with the generation of instrument raw data, with an ad-hoc compromise between calculation complexity (namely, computation time) and level 0 data representativeness. The instrument responses (point spread function and spectral response function) are built considering low level parameters such as aperture, optical aberration wave front error, slit size, detector size, as well as possible on-board binning. The positions of channel barycentre considers a nominal sampling grid (defined by designed) in association with the smile that may occur across the field of view. The spatial and spectral convolutions are applied consecutively on the high resolution radiance hypercube produced by the scene generator which is under E2ES responsibility.

The theoretical radiance as seen by a perfect instrument is then calculated. Fig. 20 illustrates radiance results obtained on a validation scene made of a checkerboard pattern including an homogeneous area producing L_{ref} radiance. The detection and video chain of FLORIS is modelled in order to introduce non uniformities and noise impacts on the raw data, and to convert the resulting signal into instrument units.
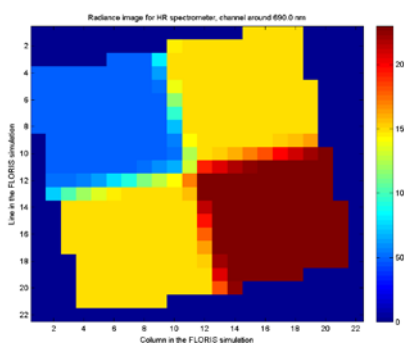
| spatial distribution of signal inside FLORIS image for HR channel located at 750 nm | spectral radiance simulated for a spatial sample looking at the part of the scene producing Lref radiance |
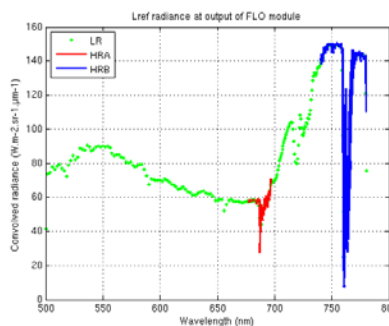
Fig. 20: Example of FLORIS radiance simulated over a validation pattern made of checkerboard

The L1B module finally processes FLORIS level 0 raw data in a standard way in order to go back to physical units. This module also integrates a very important element that generates radiometric calibration errors of various kinds. Relative spatial, relative spectral and absolute radiometric errors can in particular be introduced with adjustable levels, allowing determining later in the E2ES the sensitivity of the fluorescence retrieval on these errors. The OSS modules are compliant with OpenSF framework, so that they can be directly integrated in the E2ES. The top level parameters of the OSS are accessible in XML configuration files; they can be easily modified by the user, e.g., in the frame of a mission sensitivity analysis.

X. CONCLUSION

The outcome of this phase A/B1 study is a FLORIS concept meeting all the requirements. An optical breadboard of the HR channel called FIMAS for FLEX IMAging Spectrometer has been realised and tested. These tests have confirmed the estimated performances. The stray light generated by the instrument, and in particular the spectral stray light, is acknowledged to be a critical issue as it could affect the radiometric accuracy within the absorption band at 761 nm which is fundamental to recover the fluorescence signal. Pre-development activities are currently running on the grating roughness, on the lens and mirror superpolishing techniques to reduce further the stray light level. Optimised procedures have been defined to get the lowest possible level of contamination. Accurate methods have been defined to calibrate the FLORIS instrument BSDF. The precised knowledge of the instrument BSDF allow a correction of stray light to be performed in orbit.

XI. ACKNOWLEDGEMENT